HHS Public Access

Author manuscript

*Immunology*. Author manuscript; available in PMC 2023 July 19.

Published in final edited form as:

*Immunology*. 2022 February ; 165(2): 195–205. doi:10.1111/imm.13427.

# NLRP3 Knockout Enhances Immune Infiltration and Inflammatory Responses and Improves Survival in a Burn-Sepsis Model

**Mile Stanojcic, PhD**[*,4], **Roohi Vinaik, MD**[*,4], **Abdikarim Abdullahi, PhD**[4], **Peter Chen, PhD**[4], **Marc G Jeschke, MD PhD**[1,2,3,4]

[1]Department of Surgery, Division of Plastic Surgery, University of Toronto, Canada

[2]Department of Immunology, University of Toronto, Canada

[3]Ross Tilley Burn Centre, Sunnybrook Health Sciences Centre, Toronto, Canada

[4]Sunnybrook Research Institute, Toronto, Canada

## Abstract

Although sepsis in burn patients is a major contributor to mortality, treatments are not always effective and underlying mechanisms have yet to be completely elucidated. NLRP3 inflammasome orchestrates burn-induced, inflammatory-driven pathophysiologic processes. Here, we determined the mechanism of NLRP3 inflammasome activation on bacterial clearance and mortality in burn sepsis. We obtained tissue and blood from 30 wild-type and 30 *Nlrp3*$^{-/-}$ mice. Mice were subjected to a two-hit model of 25–30% TBSA scald burn followed by *Pseudomonas aeruginosa* wound infection 72 hours after injury. We also obtained tissue from 34 adult burn patients (≥18 years of age) with early (0–11 days post-burn) and later (≥12 days post-burn) surgical time-points and ten healthy controls. Murine studies indicated that *Nlrp3*$^{-/-}$ had 30% improved survival and bacterial clearance at the site of injury and is systemically relative to burn sepsis wild type. Greater macrophage and neutrophil infiltration occurred acutely after infection (12 hours) to the site of injury and adipose tissue. This was followed by increased macrophage and neutrophil infiltration to lymphoid organs and liver beyond the acute phase (24 and 72 hours). Interestingly, *Nlrp3* ablation increased acute systemic inflammation (IL-6, TNF-α, IL-1β). Septic burn patients had persistently increased adipose NLRP3 by-product expression beyond the acute phase that was more pronounced in late-onset sepsis. Our findings suggest that *Nlrp3* genetic ablation enhanced acute tissue-specific inflammatory responsiveness. Likely, this occurs by paradoxically increasing acute immune infiltration and inflammation with a non-persistent response. Clinically, persistent NLRP3-mediated inflammation occurs in septic versus normal burn patients and potentially detrimentally impacts patient outcomes.

**Corresponding Author**: Marc G Jeschke, MD, PhD, Director Ross Tilley Burn Centre, Sunnybrook Health Sciences Centre; Division of Plastic Surgery, Department of Surgery, Department of Immunology, University of Toronto; Sunnybrook Research Institute, 2075 Bayview Ave., Rm D704, Toronto, ON, CANADA, M4N 3M5, Tel: 416-480-6703; Fax: 416-480-6763; marc.jeschke@sunnybrook.ca.

*These authors contributed equally

**Keywords**

sepsis; burns; inflammasome; inflammation; mortality

## INTRODUCTION

The leading cause of mortality in burn patients is sepsis (1,2). Burn patients are more prone to sepsis due to loss of skin integrity and prolonged hyperinflammatory responses. The inflammatory response initiated immediately post-burn can last for several weeks to months after injury with distinct immune trajectories in these patients (3,4). Cytokines including interleukin 6 (IL-6), IL-1β, IL-10, monocyte chemoattractant protein-1 (MCP-1) and tumor necrosis factor alpha (TNF-α) are important mediators of the immune-metabolic response and play a crucial role in the complex pathophysiology underlying post-burn sepsis (4,5). Pathogens that frequently cause sepsis in burn patients, such as *Pseudomonas aeruginosa* and *Acinetobacter baumannii*, are opportunistic organisms that thrive in an immunosuppressed host (6–10). Although sepsis in thermally injured patients represents the main contributor to post-burn mortality, effective treatment is absent and underlying mechanisms are essentially unknown.

Recently, the NLRP3 inflammasome was shown to orchestrate sepsis-induced, inflammatory-driven pathophysiologic processes. The NLRP3 inflammasome is a protein complex that mediates inflammation and metabolic regulation by cleaving IL-1β and IL-18 into their bioactive forms in response to pathogens or stress (11). Assembly and/or activation of NLRP3 inflammasome is promoted by a number of damage-associated molecular patterns including ER stress (12), mitochondrial damage (13) and elevated free fatty acid levels (14–16), all of which are significantly upregulated after burns (16, 17). Originally believed to have a protective post-burn role in rodent models (18), we previously demonstrated evidence of NLRP3 activation in key immunometabolic organs after burn, including white adipose tissue, skin and liver (19–22). However, the activation and function of the NLRP3 inflammasome during burn sepsis has yet to be completely elucidated. Recent work illustrated that artemisinin administration protects against burn sepsis by attenuating inflammation and inflammatory cell infiltration in murine models (23). Additionally, another study indicated that genetic deficiency of NLRP3 resolved inflammation and increased survival in polymicrobial sepsis (24). Based on the current literature, we postulated that genetic deletion of *Nlrp3* would similarly improve outcomes in burn sepsis. Presently, we aimed to elucidate the role of a *Nlrp3* genetic deletion on bacterial clearance and survival in thermally injured septic mice. To translate our animal data into a clinical setting, we also aimed to determine whether NLRP3 inflammasome activation is augmented in severely burned septic patients during acute hospitalization.

## MATERIALS AND METHODS

### Ethics Statement:

Animal and human studies were conducted in accordance and approved by the Sunnybrook Research Institute Animal Care Committee and Research Ethics Board at Sunnybrook Hospital (Toronto, Ontario, Canada; REB#: 194–2010).

### Animals and Model.

Wild-type C57/B6 (WT) and *Nlrp3* knockout (*Nlrp3*$^{-/-}$) male mice (6–8 weeks old) were purchased from Jackson Laboratories (Bar Harbor, ME), acclimatized for a week at ambient temperature prior to initiating the study and cared for in accordance with the Guide for the Care and Use of Laboratory Animals. Mice were randomly assigned into control or burn plus infection treatment groups and researchers were blinded to the intervention. A full-thickness, third degree dorsal scald burn encompassing 25–30% total body surface area (TBSA) was induced by immersing mice in 98°C water for 10 seconds. Control mice received similar conditions excluding the burn and infection insults. All mice were included in analysis unless mortality occurred within 24-hours after burn. All tissues were harvested upon sacrifice and stored in −80°C until analysis.

### Pseudomonas Infection.

*Pseudomonas aeruginosa* (ATCC, Rockville, MD) was grown in tryptic soy agar (Sigma-Aldrich) overnight than prepared in saline to a concentration of 1.0–1.2 × $10^7$ colony-forming units (CFU). WT and *Nlrp3*$^{-/-}$ burned mice (burn+PA) received a topical infection 72-hours after burn injury, by applying 100uL on the burn area and than subsequently housed individually. All mice were sacrificed at 12- (topical infection is present systemically), 24- and 72- (sepsis) hours after infection.

### Bacterial counts.

Upon killing, lung and the central area of injury site were excised and manually homogenized in 1mL saline. Blood was obtained via cardiac puncture and centrifuged for 20 minutes at 3,000 rpm, and plasma was collected. Tissue and plasma were plated onto tryptic soy agar. Plates were grown overnight at 37°C, and PA colonies were counted to determine CFU.

### Tissue staining and flow cytometry.

Bone marrow, spleen, site of injury, liver and epididymal adipose tissue cells were used for analysis of populations of monocytes/macrophages and neutrophils. Samples were digested in collagenase (Life Technologies), Fc blocked (anti-mouse CD16/CD32, BD Pharmingen) on ice for 15 minutes and stained with monoclonal antibodies on ice for 30 minutes. Samples were then washed and analyzed using BD LSR II Special Order System (BD Biosciences, San Jose, CA, USA). Cells were gated on FSC-A and SSC-A, followed by doublet exclusion (FSC-W x FSC- H, SSC-W x SSC-H). The total percentage of monocytes/macrophages and neutrophils were identified using the following flurochrome-conjugated antibodies: anti-CD45 (anti- mouse PE-Cyanine7, eBioscience), anti-CD11b (anti-mouse

Alexa APC-eFluor® 780, eBioscience), anti-F4/80 (anti-mouse FITC, eBioscience), anti-CD11c (anti-mouse PerCP-Cyanine5.5, eBioscience) and anti-GR-1 (anti-mouse PE, eBioscience) in accordance with the manufacturer's flow cytometry protocol. The gating strategy for assessing innate immune cell distributions included leukocytes initially gated based on granularity and CD45 (side scatter x CD45), followed by size (forward scatter). Gated cells were stained for cell surface markers for monocytes and macrophages (CD11b+/F4/80+) or neutrophils (CD11b+/GR-1+). Monocytes/macrophages were also gated on CD45+/CD11b+/F4/80+/Ly6C+ populations and showed similar cell proportions and trajectories so all subsequent analysis was continued using CD45+/CD11b+/F4/80+ gating for this population.

### Gene expression using RT-PCR.

RNA was extracted from rodent liver and adipose tissue and excised human adipose tissue from burn patients using Trizol (Invitrogen, CA, USA). Reverse transcription were performed with high-capacity cDNA reverse transcription kit and (ABI, MA, USA). RT-PCR was performed using TaqMan® Fast Advanced Master Mix with the following primers *IL-1β* (Mm00434228_m1, *Caspase-1* (Mm00438023_m1, ThermoFisher), *IL-18* (Mm00434226_m1, ThermoFisher), *Caspase-3* (Mm01195085_m1, ThermoFisher), *Caspase-8* (Mm01255716_m1, ThermoFisher), *Actb* (Mm02619580_g1, *BiP* (Mm00517691_m1, ThermoFisher), in accordance with manufacturers protocol. Gene expression was expressed relative to β-actin. Due to inter-species variability between WT and *Nlrp3*$^{-/-}$ control concentrations, all values are presented as a ratio relative to the mean concentration of species- specific controls for a given primer.

### Western blotting.

Proteins from rodent liver and adipose tissues were extracted in RIPA buffer containing phosphatases and proteases inhibitor cocktails (Roche). Protein concentrations were determined by the BCA protein assay kit (Pierce, Mississauga, ON, Canada). Proteins were resolved by SDS-PAGE followed by western blotting using the following antibodies at 1:500– 1:1000 concentration: IL-1β (Cell Signaling, MA, USA), Caspase-1 (Abcam, MA USA), IL-18 (Abcam, MA USA), ASC (Adipogen, CA, USA), NF-κB (Cell Signaling, MA, USA), phospho- eIF2α (Cell Signaling, MA, USA), phospho-JNK (Cell Signaling, MA, USA), BiP (Cell Signaling, MA, USA) and GAPDH (Cell Signaling, MA, USA). Species appropriate secondary antibodies conjugated to horseradish peroxidise (BioRad, Mississauga, ON, Canada) were used and proteins visualized by enhanced chemiluminescence using the BioRad ChemiDoc MP Imaging System. Band intensities were detected, normalized and quantified with the ChemiDoc and Image Lab 5.0 software (BioRad Laboratories, Hercules, CA). Antibody concentrations are expressed relative to GAPDH. Due to inter-species variability between WT and *Nlrp3*$^{-/-}$ control concentrations, all values are presented as a ratio relative to the mean concentration of species- specific controls for a given antibody.

### Cytokine profiling.

EDTA-anticoagulated blood samples were collected from all mice at the time of sacrifice and stored in −80°C until analysis. Plasma samples were used to compare inflammatory,

chemokine and immune mediators between groups using a Multiplex platform (Millipore, MA). Experimental kits were all conducted in accordance with manufacturers' protocol. Raw data was processed using Millipore Analyst software. All values are presented as mean ± SEM and expressed in pg/ml.

### Patient samples and gene expression in adipose tissue.

Adult burn patients (≥ 18 years of age) admitted to the Ross Tilley Burn Centre at Sunnybrook Hospital (Toronto, Canada) or patients undergoing elective surgery were consented pre-operatively for tissue collection and inclusion. Patients were excluded if the admission was elective or if it was a readmission. We analyzed 34 adult burned patients (≥ 18 years of age) white adipose tissue (WAT) obtained from both early (0–11 days post burn) and later (≥12 days post burn) surgical time points (refer to supplemental table 1 for detailed patient demographics). Sepsis was defined prospectively by the staff burn surgeons based on the clinical presentation of the patient but also in accordance with the American Burn Association (ABA) guidelines as well as new Critical Care Guidelines (23,24). Ten healthy controls were used to compare burn patients to normal tissue. Adipose tissue was immediately transferred to the laboratory and frozen (−80°C) until time of analysis. Specific primers yielding single specific amplicon were chosen for *NLRP3*, *IL1β*, *Caspase 1* and *IL18*. RT-PCR was performed with Sybr green Supermix (Biorad, CA, USA).

### Statistical Analysis.

All data are represented as mean ± SEM. Survival curves were analyzed using the log-rank (Mantel–Cox) test. Statistical analysis was performed using student's t-test, one and two-way ANOVA with Tukey's multiple correction tests to compare groups, where appropriate. All graphs were created using Graphpad Prism 6.0 (San Diego, CA) and analyzed statistically using SPSS 20 (IBM Corp., NY, NY), with significance accepted at $p < 0.05$ (*), $p < 0.01$ (**), $p < 0.001$ (***) and $p < 0.05$ (#), $p < 0.01$ (##), $p < 0.001$ (###), where appropriate.

## RESULTS

### Post-burn septic *Nlrp3*$^{-/-}$ have improved survival and bacterial clearance compared to WT mice

Initially, we compared mortality in our model of burn plus sepsis (*Pseudomonas* (PA) seeding model) versus controls, demonstrating a significantly greater mortality rate of 40% occurring as early as 3–4 days post-infection (Mantel-Cox = 5.3, p=0.021, Fig.1A) (25). This is comparable to the clinical scenario; burn patients with sepsis have a 30–40% mortality rate (23,24). Ablation of *Nlrp3* resulted in 30% improvement in overall survival (90%) relative to WT burn+PA (Mantel-Cox = 3.9, p=0.047; Fig.1A). Unlike septic WT, *Nlrp3*$^{-/-}$ burn+PA mice reached their end point significantly later (8 days) after infection ($p<0.05$), indicating not only improved but also prolonged survival.

Since bacterial colonization at the site of injury is a key early event in development of clinical sepsis, we compared bacterial counts at 72 hours after infection (henceforth referred to as 'infectious period' – the correlate of early sepsis in our burn +infection rodent model)

(Fig.1B–C). Interestingly, *Nlrp3*$^{-/-}$ burn+PA had significantly lower proportions at the site of injury ($p<0.05$) relative to WT burn+PA mice, suggesting that wound colonization was exclusive to WT. Furthermore, *Nlrp3*$^{-/-}$ burn+PA plasma bacterial counts appeared lower than WT although this was not significant. Although we cannot conclude that systemic bacterial dissemination was lower in *Nlrp3*$^{-/-}$, wound bacterial colonization has an important role in impaired wound healing and increased risk of systemic sepsis.

We next wanted to determine if these improvements were attributed to improved innate immune cell populations at the site of injury. Flow cytometric analysis acutely after infection (12-hours) revealed that *Nlrp3*$^{-/-}$ had increased monocyte/macrophage proportions at the site of injury relative to controls ($p<0.01$) and WT burn+PA ($p<0.05$, Fig.1D–E). This was also observed at 24-hours. During the infections period (72 hours), increased macrophages at the site of injury were common to both WT and *Nlrp3*$^{-/-}$ relative to inherent controls ($p<0.01$, Fig.1D). Notably, increases in macrophages in WT burn+PA were comparable to that of *Nlrp3*$^{-/-}$ burn+PA during the early time point (12-hours), suggesting a delayed response to infection. A similar trajectory to macrophages was observed in *Nlrp3*$^{-/-}$ burn+PA neutrophils, with a greater proportion relative to WT burn+PA at 24-hours (14.3% vs. 2.5%; $p<0.01$, Fig.1E). The absence of an abundant neutrophil population in knockouts during the infectious period suggests a decreased immunological demand from pathogenic intrusion. Collectively, these findings suggest that *Nlrp3*$^{-/-}$ mice survive post-burn sepsis better than WT counterparts in part due to improved macrophage and neutrophil recruitment to the site of injury and containment of bacterial spread.

### *Nlrp3*$^{-/-}$ mice have increased macrophage and neutrophil infiltration after infection independent of lymphoid organs.

Given that improved bacterial clearance from the site of injury could have occurred as a result of greater macrophage and neutrophils proportions, we next investigated the possible origins of these infiltrated immune cells. When comparing immune cell production in the peripheral lymphoid organs, WT burn+PA mice show an overall increase in spleen from infection (12-hours) to sepsis (72-hours) progression. Percentage of macrophages in the spleen also increased in the WT burn+PA group at later time-points (Fig.2A–B). A similar trend was observed in neutrophils. When comparing the bone marrow monocyte/macrophage population in WT burn+PA, there was a gradual increase that was significantly higher beyond the acute phase (Fig.2C). Interestingly, neutrophils in the bone marrow of *Nlrp3*$^{-/-}$ had a greater proportion early and late after infection (Fig.2D). Taken together, acute infiltration at the site of injury was most likely not attributed to immune expansion in the lymphoid organs.

Extending this analysis to the liver and adipose tissue, the lack of *Nlrp3* resulted in increasingly greater hepatic macrophages and neutrophils (Fig.2E–F). *Nlrp3*$^{-/-}$ burn+PA had approximately 2-times more macrophages ($p<0.01$) and neutrophils ($p<0.01$) than WT counterparts at 24 and 72-hours (Fig.2E–F). Unlike the gradual increases in hepatic innate immune cell populations in *Nlrp3*$^{-/-}$ burn+PA mice, the adipose tissue supported a unique, acute responsiveness to insult relative to WT. At 12-hours after infection, *Nlrp3*$^{-/-}$ burn+PA had a 4-fold increase in macrophages ($p<0.05$) and nearly 6-fold increase in neutrophils

(p<0.05), relative to WT burn+PA. WT burn+PA demonstrated macrophage and neutrophil increases later at 72-hours after infection (Fig.2G–H). Thus, these findings suggest that the adipose tissue of *Nlrp3*$^{-/-}$ exclusively elicits an immediate response to combat pathogenic invasion and prevent bacterial spread. These observations occurred secondary or later in liver and lymphoid organs. As the main immune modulators after burn trauma (26), we next determined the effects of increased innate immune cell populations on ER stress and inflammasome component activity in adipose tissue and liver.

## Increased adipose tissue inflammasome component activation, ER stress and cell death early after infection in *Nlrp3*$^{-/-}$ burn+PA mice

The role of adipose tissue has largely been neglected in the context of infectious diseases. When comparing inflammasome activity in infectious groups acutely after insult, *Nlrp3*$^{-/-}$ burn+PA showed increased ASC, mature IL-1β and IL-18 protein expression relative to WT burn+PA (p<0.05, Fig.3A–C). Consistent with this, *Nlrp3*$^{-/-}$ also manifested greater NF-κB and (p<0.05) and cleaved Caspase-1 (p<0.01) expression early after infection relative to WT burn+PA (12 & 24-hours, respectively, Fig.3D–E). It is important to note that enhanced inflammasome components such as ASC are not necessarily indicative of greater activation, but increased expression of inflammasome components is possibly reflective of enhanced macrophage infiltration in adipose tissue of *Nlrp3*-deficient mice. Furthermore, contribution of other inflammasomes and ER-stress induced inflammation can potentiate inflammasome-independent cleavage of cytokines (i.e. IL-1β), providing a rationale for these findings (27). Indeed, the ER stress marker BiP also showed significantly greater expression in *Nlrp3*$^{-/-}$ relative to controls at 12 and 24 hours (Fig.3F). Lastly, cleaved caspase-3 was significantly higher acutely after infection in *Nlrp3*$^{-/-}$ burn+PA group relative to WT burn+PA suggesting greater apoptosis (Fig.3I). Interestingly, similar peaks in Caspase-3 protein expression in WT burn+PA mice occurred later at 72-hours after infection relative to knockout counterparts (p<0.05), suggesting a delayed cell death response contributing to impaired bacterial clearance. Similar effects were observed in adipose tissue gene expression with increases in the *Nlrp3*$^{-/-}$ infectious group relative to WT counterparts, however it was most pronounced at the 72-hour time point (Supplemental Fig.1A–F).

We next compared protein expression in the liver, another key immunometabolic organ. Unexpectedly, we did not observe the same acute responsiveness to infectious insult in *Nlrp3*$^{-/-}$ as in adipose tissue. Overall, the WT burn+PA group had increased inflammasome component and cell death expression. Specifically, inflammasome activity in WT showed the greatest difference at 24-hours after infection (Supplemental Fig.2). To a lesser extent, hepatic gene expression revealed a similar trajectory for the aforementioned data (Supplemental Fig.1G–L). In summary, consistent with immune cell infiltration previously shown, the absence of NLRP3 inflammasome resulted in acute responsiveness of the adipose tissue to infection characterized by greater ER stress, cell death and alternative inflammatory pathway activation; for example, ASC-dependent activation of non-inflammasome cytokines (e.g. IL-6, TNF-α) via NF-κB (28). With this in mind, we next determined whether systemic mediators are driving these increases in tissue in the absence of increased lymphoid macrophage infiltration.

### Acute and non-persistent systemic inflammation and chemokine response in *Nlrp3*$^{-/-}$ burn+PA mice

Next, we aimed to elucidate whether there were alterations in systemic inflammatory processes between WT and *Nlrp3*$^{-/-}$ burn+PA mice which could account for differential immune mobilization and tissue inflammation. We noted that *Nlrp3*$^{-/-}$ exhibited greater acute responses for inflammatory, chemokine and immune mediating cytokines, similar to the adipose tissue-specific expression profile for inflammatory cytokines. All integral pro-inflammatory cytokines were significantly increased in the *Nlrp3*$^{-/-}$ burn+PA group relative to WT burn+PA acutely (12-hours), including IL-6, TNF-α, and IL-1β (Fig.4A–C). Notably, IL-6 had the most pronounced elevation in acute phase response (WT burn+PA = 183 pg/ml vs. *Nlrp3*$^{-/-}$ = 1128 pg/ml). Consistent with the observed increase in inflammatory cytokines, chemokine and other immune mediator analysis in *Nlrp3*$^{-/-}$ revealed greater concentrations at 12-hours after infection relative to WT burn+PA (Fig.4D–I). Additional cytokines that were analyzed can be found in Supplemental Fig. 3. Thus, *Nlrp3*$^{-/-}$ have greater inflammatory and chemokine responses characterized by acute elevation after PA infection in the absence of aberrant and prolonged inflammatory response to bacterial challenge.

### Adult septic burn patients have prolonged increases in NLRP3 inflammasome gene expression in white adipose tissue beyond the acute phase

In order to determine if our present findings in rodents are translatable to patients and whether the adipose tissue is in fact a critical early mediator of insult, we assessed NLRP3 inflammasome gene expression in white adipose tissue of controls, non-septic and septic burn patients. Our findings revealed a temporal trend that was consistent with WT mice during the course of infection and sepsis. Early after burn (0–11 days), the non-sepsis patient group had a fairly consistent increase in gene expression relative to controls for *IL-1β*, *IL-18* and *NLRP3* ($p<0.01$, Fig.5A–D). At later time points (≥12 days), inflammasome component expression returned to baseline or control concentrations. Interestingly, septic burn patients had significantly greater gene expression at later time points relative to controls (*IL-1β*, *Caspase-1* and *NLRP3*, $p<0.05$) and non-sepsis burn patients (*IL-1β*, *IL-18* and *NLRP3*, $p<0.05$). When exclusively looking at septic burn patients, late-onset sepsis (≥12 days post-burn) had greater gene expression relative to controls and non-septic burns (*IL-1β*, *Caspase-1*, *IL-18* and *NLRP3*, $p<0.05$, Fig.5E–H). Collectively, this data suggests that septic burn patients have increased NLRP3 inflammasome gene expression in white adipose tissue at later time points. Potentially, persistence of acute phase inflammation is associated with increased risk of sepsis and as a result, poor outcomes and death (Supplemental Table 1).

## DISCUSSION

NLRP3 inflammasome is the central regulator of inflammation in burn trauma and has been shown to have an integral role in various post-burn processes, including wound healing, regulation of lipid turnover and glucose metabolism (29–31). While potentially protective in non-septic burns, genetic deficiency of *Nlrp3* and reduced inflammasome activation improved outcomes in sepsis via resolution of inflammation and pyroptosis. Therefore, the question arises: is lack of *Nlrp3* detrimental or beneficial in a burn-sepsis model? To our

knowledge, our present findings are the first to demonstrate that absence of *Nlrp3* may have a protective role specific to burn sepsis via enhanced induction of an acute compensatory systemic and adipose tissue-specific inflammatory response. This immediate compensatory response was unique to adipose tissue and was not observed in the liver or other lymphoid organs, thus supporting the imperative role that the adipose tissue plays in responding to post-burn infection and sepsis.

An important feature seen in *Nlrp3*$^{-/-}$ was the acute responsiveness of pro-inflammatory factors and chemokines and accelerated recruitment of neutrophils and macrophages to adipose tissue. Despite this early upregulation in adipose inflammasome-related factors (e.g. ASC, IL-1β) and systemic inflammatory mediators (e.g. IL-6, TNF-α, IL-1β), chemokines (e.g. MIP-1α) and immune mediators (e.g. G-CSF), *Nlrp3*$^{-/-}$ exhibited compatible and in certain cases lower levels of the aforementioned markers compared to WT by 72 hours. Interestingly, lack of *Nlrp3* may indirectly affect early monocytic cell lineages via enhanced production of G-CSF and IL-6 acutely. Together, these factors promote activation of STAT3 and neutrophil prioritization in bone marrow, which we see in *Nlrp3*$^{-/-}$ (32). Although lack of *Nlrp3* improves innate cell infiltration and enhances early inflammatory responses, we showed resolution by 72 hours. Clinically, non-septic thermally injured patients exhibited similar gradual decreases in adipose tissue inflammasome gene expression to baseline compared to septic patients. However, a key caveat in this study is the difference in cellularity between various rodent and human samples. Although we focus on the role of NLRP3 activation in the various outcomes, altered immune cell infiltration and activity could have an important role as well. However, while we cannot attribute increased infection susceptibility to alterations in inflammasome genes *per se*, these results suggest that timing and magnitude of inflammation specifically in adipose tissue may be a key line of investigation. Another potential limitation is that normal wound closure has an important role in sepsis, and persistence of open wounds rather than altered NLRP3 could contribute to poor outcomes. However, NLRP3 in turn has an important effect in normal wound healing after burn and therefore could have a role, albeit one related more to healing.

Another important question arises: how do *Nlrp3*$^{-/-}$ mice demonstrate enhanced production of inflammasome byproducts (e.g. mature IL-1β)? While NLRP3 inflammasome activation is a key pathway for IL-1β and Caspase-1 cleavage and maturation, studies suggest potential NLRP3-independent inflammatory pathways. For example, situations resulting in induction of ER stress such as burns promote Caspase-8-dependent cleavage of IL-1β, while NF-κB activation stimulates pro-IL-1β expression (27,33). Additionally, increasing bacterial challenge enhances TNF-α signaling in a recent study investigating *Mycobacterium*-induced regulated cell death (34). *Nlrp3*$^{-/-}$ have increased TNF-α in plasma, NF-κB, Caspase-8 and inflammation (IL-1β) in adipose tissue acutely, supporting the notion that *Nlrp3* deficient mice knockouts may be utilizing a multitude of processes that ultimately culminate in a common goal of acute inflammation and immune cell recruitment for pathogen clearance. It is important to note that while compensatory inflammatory pathways (e.g. Caspase-8 and TNF-α signaling) could be activated in *Nlrp3*$^{-/-}$, we cannot exclude contribution from other NLRs such as NLRP1 (35). However, to our knowledge NLRP3 is the key inflammasome activated in burns. Taken together, we showed that despite genetic deletion of *Nlrp3*, there

is still evidence of acute compensatory inflammation *in vivo*, underscoring the evolutionary importance of acute versus chronic post-trauma inflammation.

To conclude, the unexpected onset of an exacerbated acute pro-inflammatory state post burn and infection due to the absence of the NLRP3 inflammasome is rather paradoxical. It induces greater inflammation during the acute phase to contain the bacterial challenge, and these effects return back to baseline and do not persist. Prior burn studies have highlighted the importance of early inflammation and here, we similarly illustrate that acute inflammation is required and imperative in burn-sepsis as well. Therefore, instead of perceiving the inflammasome as an inducer of inflammation, in the context of sepsis we should redefine the inflammasome as a "gauge" moderating inflammation to ensure bacterial challenges are mitigated acutely to avoid inflammatory persistence. The differential pro-inflammatory response illustrated by both enhanced cellular recruitment to the site of injury and adipose tissue and the elevated effector molecule expression underscores an important putative role for NLRP3 inflammasome in determining burn sepsis clinical outcomes.

## Supplementary Material

Refer to Web version on PubMed Central for supplementary material.

## Acknowledgements

We would like to thank Drs. Tracy Toliver-Kinsky and Andrew Simor for their insight and guidance with the two-hit model. We would also like to thank Alexandra Parousis for her technical assistance and the clinical and research staff at Ross Tilley Burn Centre. Mile Stanojcic is the recipient of the Canadian Institute of Health Research Frederick Banting and Charles Best doctoral research award.

**Conflicts of Interest and Source of Funding:**

This study was supported by -Canadian Institutes of Health Research # 123336. CFI Leader's Opportunity Fund: Project # 25407 NIH RO1 GM087285-01

## References

1. Williams FN, Herndon DN, Hawkins HK, et al. : The leading causes of death after burn injury in a single pediatric burn center. Crit Care 2009; 13:R183. [PubMed: 19919684]
2. Church D, Elsayed S, Reid O, et al. : Burn wound infections. Clin Microbiol Rev 2006; 19:403–434. [PubMed: 16614255]
3. Finnerty CC, Jeschke MG, Herndon DN, et al. : Temporal cytokine profiles in severely burned patients: a comparison of adults and children. Mol Med 2008; 14:553–560. [PubMed: 18548133]
4. Jeschke MG, Mlcak RP, Finnerty CC, et al. : Burn size determines the inflammatory and hypermetabolic response. Crit Care 2007; 11:R90. [PubMed: 17716366]
5. Murphy TJ, Paterson HM, Kriynovich S, et al. : Linking the "two-hit" response following injury to enhanced TLR4 reactivity. J Leukoc Biol 2005; 77:16–23. [PubMed: 15496450]
6. O'Riordain MG, O'Riordain DS, Molloy RG, et al. : Dosage and timing of anti-TNF-alpha antibody treatment determine its effect of resistance to sepsis after injury. J Surg Res 1996; 64:95–101. [PubMed: 8806480]
7. Lavrentieva A, Voutsas V, Konoglou M, et al. : Determinants of Outcome in Burn ICU Patients with Septic Shock. J Burn Care Res 2017; 38:e172–e179. [PubMed: 27003623]

8. Hotchkiss RS, Monneret G, Payen D: Immunosuppression in sepsis: a novel understanding of the disorder and a new therapeutic approach. Lancet Infect Dis 2013; 13:260–268. [PubMed: 23427891]
9. Hodle AE, Richter KP, Thompson RM: Infection control practices in U.S. burn units. J Burn Care Res 2006; 27:142–151. [PubMed: 16566557]
10. Falcone M, Russo A, Iacovelli A, Restuccia G, Ceccarelli G, Giordano A, et al. . Predictors of outcome in ICU patients with septic shock caused by Klebsiella pneumoniae carbapenemase-producing K. pneumoniae. Clin Microbiol Infect 2016; 22:444–50. [PubMed: 26850826]
11. Nichols DP, Caceres S, Caverly L, et al. : Effects of azithromycin in Pseudomonas aeruginosa burn wound infection. J Surg Res 2013; 183:767–776. [PubMed: 23478086]
12. Li W, Cao T, Luo C, et al. : Crosstalk between ER stress, NLRP3 inflammasome, and inflammation. Appl Microbiol Biotechnol 2020; 104:6129–6140. [PubMed: 32447438]
13. Martinon F, Burns K, Tschopp J: The inflammasome: a molecular platform triggering activation of inflammatory caspases and processing of proIL-beta. Mol Cell 2002; 10:417–426. [PubMed: 12191486]
14. Bronner DN, Abuaita BH, Chen X, et al. : Endoplasmic Reticulum Stress Activates the Inflammasome via NLRP3- and Caspase-2-Driven Mitochondrial Damage. Immunity 2015; 43:451–462. [PubMed: 26341399]
15. Shimada K, Crother TR, Karlin J, et al. : Oxidized mitochondrial DNA activates the NLRP3 inflammasome during apoptosis. Immunity 2012; 36:401–414. [PubMed: 22342844]
16. Wen H, Gris D, Lei Y, et al. : Fatty acid-induced NLRP3-ASC inflammasome activation interferes with insulin signaling. Nat Immunol 2011; 12:408–415. [PubMed: 21478880]
17. Song J, Finnerty CC, Herndon DN, et al. : Severe burn-induced endoplasmic reticulum stress and hepatic damage in mice. Mol Med 2009; 15:316–320. [PubMed: 19603103]
18. Bogdanovic E, Kraus N, Patsouris D, et al. : Endoplasmic reticulum stress in adipose tissue augments lipolysis. J Cell Mol Med 2015; 19:82–91. [PubMed: 25381905]
19. Stanojcic M, Chen P, Harrison RA, et al. : Leukocyte infiltration and activation of the NLRP3 inflammasome in white adipose tissue following thermal injury. Crit Care Med 2014; 42:1357–1364. [PubMed: 24584061]
20. Stanojcic M, Abdullahi A, Rehou S, et al. : Pathophysiological response to burn injury in adults. Ann Surg 2018; 267(3):576–584. [PubMed: 29408836]
21. Long H, Xu B, Luo Y, Luo K: Artemisinin protects mice agains burn sepsis through inhibiting NLRP3 inflammasome activation. Am J Emerg Med 2016;34:772–777. [PubMed: 26830216]
22. Vinaik R, Abdullahi A, Barayan D, Jeschke MG: NLRP3 inflammasome activity is required for wound healing after burns. Transl Res 2020;217:47–60. [PubMed: 31843468]
23. Vinaik R, Stanojcic M, Jeschke MG: NLRP3 Inflammasome Modulates Post-Burn Lipolysis and Hepatic Fat Infiltration via Fatty Acid Synthase. Sci Rep 2018;8:15197. [PubMed: 30315247]
24. Lee S, Nakahira K, Dalli J, et al. : NLRP3 Inflammasome Deficiency Protects against Microbial Sepsis via Increased Lipoxin B4 Synthesis. Am J Respir Crit Care Med 2017;196(6):713–726. [PubMed: 28245134]
25. Greenhalgh DG, Saffle JR, Holmes JH, et al. : American Burn Association consensus conference to define sepsis and infection in burns. J Burn Care Res 2007; 28:776–790. [PubMed: 17925660]
26. Singer M, Deutschman CS, Seymour CW, et al. : The Third International Consensus Definitions for Sepsis and Septic Shock (Sepsis-3). JAMA 2016; 315:801–810. [PubMed: 26903338]
27. Stevenson JM, Gamelli RL, Shankar R: A Mouse Model of Burn Wounding and Sepsis. In: DiPetro LA, Burns AL (eds) Wound Healing. Methods in Molecular Medicine, vol 78. Humana Press, Totowa, NJ.
28. Xiu F, Stanojcic M, Diao L, et al. : Stress hyperglycemia, insulin treatment, and innate immune cells. Int J Endocrinol 2014; 486403.
29. Gurung P and Kanneganti T-D: Novel Roles for Caspase-8 in IL-1β and Inflammasome Regulation. Am J Pathol 2015;185(1):17–25. [PubMed: 25451151]

30. Barker BR, Taxman DJ, Ting JP-Y: Cross-regulation between the IL-1β/IL-18 processing inflammasome and other inflammatory cytokines. Curr Opin Immunol 2011;23(5):591–597. [PubMed: 21839623]

31. Vinaik R, Barayan D, Jeschke MG: NLRP3 Inflammasome in Inflammation and Metabolism: Identifying Novel Roles in Postburn Adipose Dysfunction. Endocrinology 2020:161(9).

32. Gardner JC, Noel JG, Nikolaidis NM, et al. : G-CSF drives a posttraumatic immune program that protects the host from infection. J Immunol 2014;192(5):2405–2417. [PubMed: 24470495]

33. He Y, Hara H, Núñez G: Mechanism and Regulation of NLRP3 Inflammasome Activation. Trends Biochem Sci 2016;41(12):1012–1021. [PubMed: 27669650]

34. Roca FJ, Ramakrishnan L: TNF dually mediates resistance and susceptibility to mycobacteria via mitochondrial reactive oxygen species. Cell 2013; 153:521–534. [PubMed: 23582643]

35. Esquerdo KF, Sharma NK, Brunialti MKC, et al. : Inflammasome gene profile is modulated in septic patients, with a greater magnitude in non-survivors. Clin Exp Immunol 2017;189(2):232–240. [PubMed: 28369745]

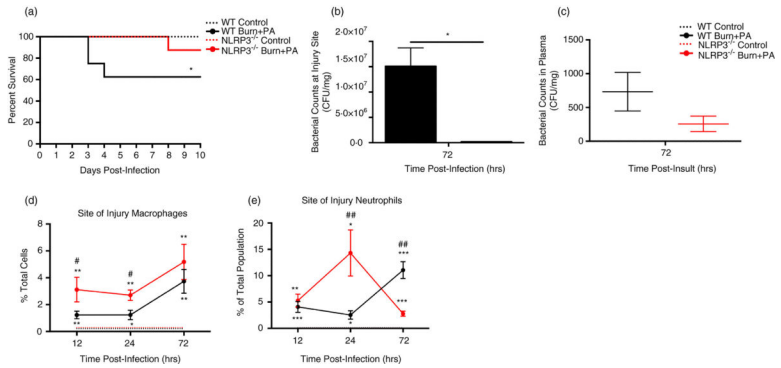


**Figure 1. Nlrp3 knockout improves survival via immune infiltration and bacterial clearance at the site of injury.**

**A,** Kaplan-Meier survival curve of WT (control and burn+PA) and *Nlrp3*$^{-/-}$ (control and burn+PA) mice relative to days post infection (n = 10 per group). **B-C**, Analysis of bacterial counts during the infectious period (72 hours post-infection) in WT and *Nlrp3*$^{-/-}$ mice for site of injury and plasma, expressed as colony-forming units per gram of tissue. **D**,**E** Temporal distribution percent of total population of macrophage and neutrophils for WT and *Nlrp3*$^{-/-}$ controls and burn+PA groups at 12, 24 and 72-hours after infection. Dotted lines represent controls (WT and *Nlrp3*$^{-/-}$) and solid lines are burn plus PA infection groups (WT burn+PA and *Nlrp3*$^{-/-}$ burn+PA). Data presented as mean ± SEM. ***** = significant difference between strain-specific controls vs. burn+PA, **#** = significant difference between WT burn+PA vs. *Nlrp3*$^{-/-}$ burn+PA, (n=5/group). */# $p<0.05$, **/## $p<0.01$ and ***/### $p<0.001$. Each flow plot is representative of macrophage population for one mouse/genotype.

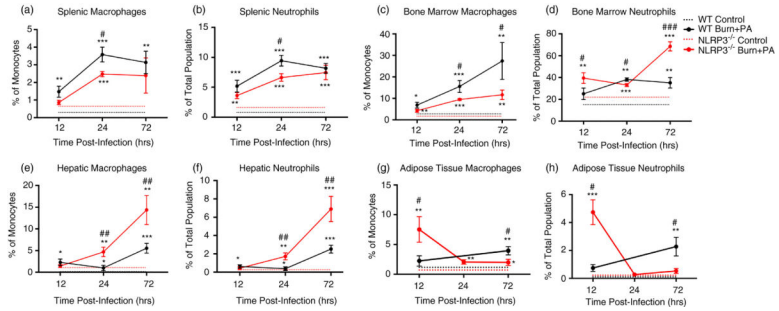


**Figure 2. Flow cytometric analysis of innate immune cells in lymphoid organs and infection infiltration tissues.**

**A-D,** Temporal analysis of lymphoid organs (spleen and bone marrow) for monocyte/macrophage and neutrophils ($CD45^+/CD11b^+/GR\text{-}1^+$) of control and burn+PA for each WT and *Nlrp3*$^{-/-}$ strains. **E, F**, Hepatic macrophages and neutrophils in *Nlrp3*$^{-/-}$ burn+PA revealed a progressively increased infiltration of immune cells beyond the acute time point (12-hours). **G, H**, Adipose tissue of *Nlrp3*$^{-/-}$ burn+PA group exclusively supported an acute elevation in proportion of macrophage and neutrophils acutely after infection (12-hours) and returned back to baseline at later time points relative to WT infectious counterparts. Dotted lines represent controls (WT and *Nlrp3*$^{-/-}$, n = 5 per genotype) and solid lines are burn plus PA infection groups (WT burn+PA and *Nlrp3*$^{-/-}$ burn+PA, n = 5 per genotype). Data presented as mean ± SEM, ***** = significant difference between strain-specific controls vs. burn+PA, **#** = significant difference between WT burn+PA vs. *Nlrp3*$^{-/-}$ burn+PA, (n=5/group). */# $p<0.05$, **/## $p<0.01$ and ***/### $p<0.001$.

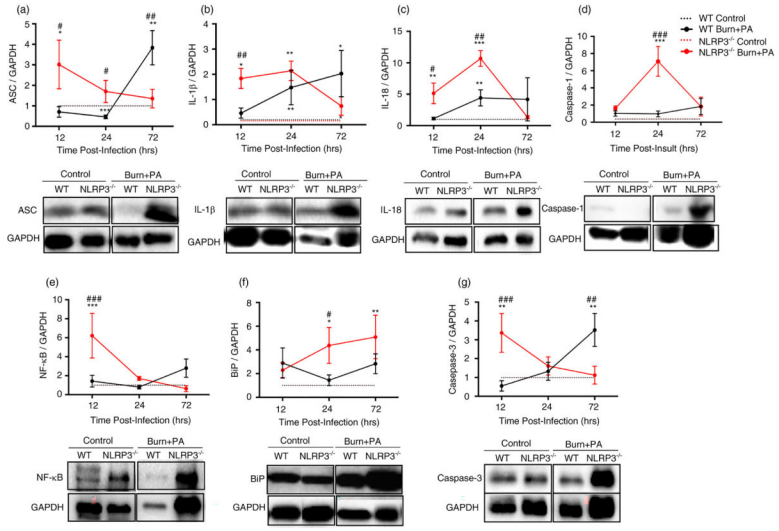


**Figure 3. Increased NLRP3 inflammasome component, ER stress and cell death expression acutely after infection in adipose tissue of *Nlrp3*$^{-/-}$ mice.**

Adipose tissue western blot analysis at 12, 24 and 72-hour time points and representative images. This includes NLRP3 inflammasome components: **A-E**, ASC (representative images = 12-hours after infection), IL-1β (12-hours after infection), IL-18 (12-hours after infection), cleaved caspase-1 (p20 subunit) (24-hours after infection) and NF-κB (p65 subunit) (24-hours after infection. **F**, ER stress protein expression was measured for BiP (24 hours after infection). Markers of apoptosis included **G**, cleaved caspase-3 (17/19 kDa subunit) (12 hours after infection). Dotted lines represent controls (WT and *Nlrp3*$^{-/-}$) and solid lines are burn plus PA infection groups (WT burn+PA and *Nlrp3*$^{-/-}$ burn+PA). Data presented as mean ± SEM and n = 5 per group. ***** = significant difference between strain-specific controls vs. burn+PA, **#** = significant difference between WT burn+PA vs. *Nlrp3*$^{-/-}$ burn+PA, */# $p<0.05$, **/## $p<0.01$ and ***/### $p<0.001$. Each blot is representative of one mouse per treatment/genotype and was conducted on the same gel in pairs for a given antibody.

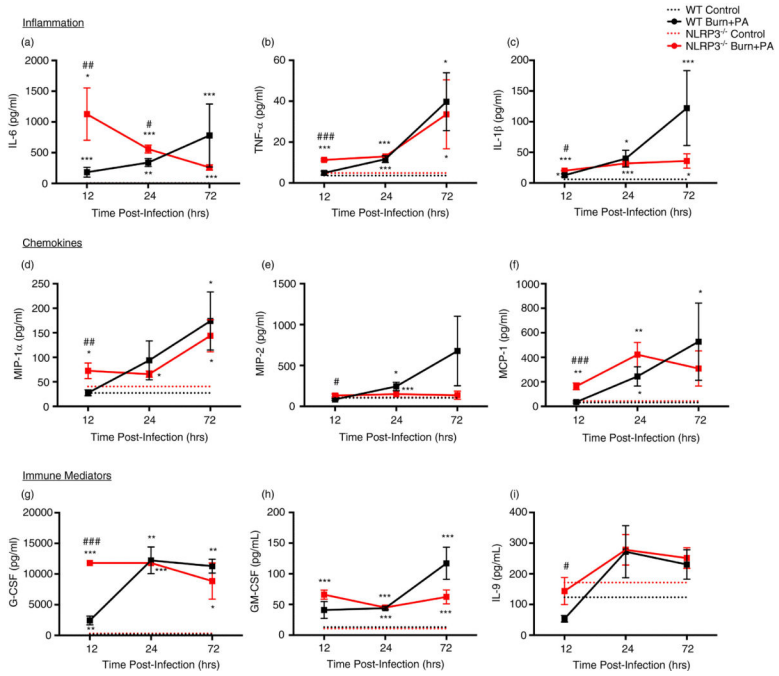


**Figure 4: Greater acute and short-lived inflammation and chemokine concentrations in systemic circulation of *Nlrp3*$^{-/-}$ mice.**

Plasma cytokine profiling of control (n = 5 per genotype/time) and burn+PA mice for WT (n = 5 per group/time) and *Nlrp3*$^{-/-}$ (n = 5 per group/time) strains at 12, 24 and 72-hours after infection. **A-C**, Cytokines that were used in the analysis included pro-inflammatory, **D-F**, chemokines, and **G-I**, immune mediators. Dotted lines represent controls (WT and *Nlrp3*$^{-/-}$) and solid lines are burn plus PA infection groups (WT burn+PA and *Nlrp3*$^{-/-}$ burn+PA). Data presented as mean ± SEM, * = significant difference between strain-specific controls vs. burn+PA, # = significant difference between WT burn+PA vs. *Nlrp3*$^{-/-}$ burn+PA. */# p<0.05, **/## p<0.01 and ***/### p<0.001

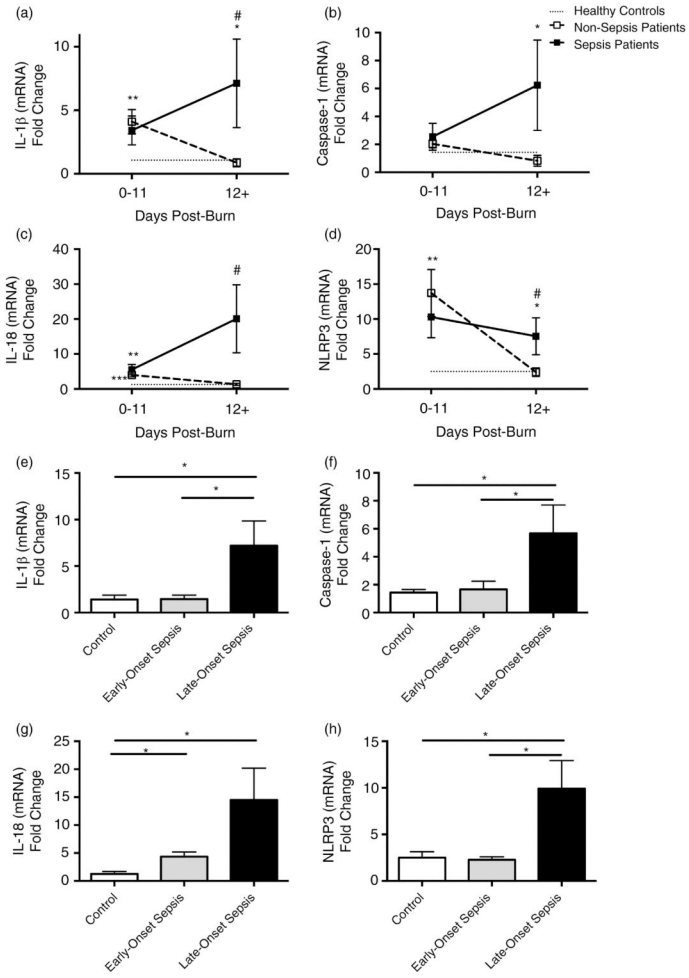


**Figure 5. Prolonged elevation of acute phase NLRP3 inflammasome gene expression in adult septic burn patients.**

Gene expression in white adipose tissue of healthy controls (n=10), non-sepsis (n=15) and sepsis (n=19) adult burn patients during the course of hospital stay (0–11 and 12+ days post burn). Primers included in the analysis were **A**, IL-1β, **B**, Caspase-1, **C**, IL-18, and **D**, NLRP3. Septic burn patients were further stratified into early (0–11 days) and late (≥12 days post burn) sepsis for (E) *IL-1β*, (F) *Caspase-1*, (G) *IL-18* and (H) *NLRP3*. Dotted lines represent healthy controls, dashed lines are burn patients and solid lines are septic burn patients. Data presented as mean ± SEM, ***** = significant difference between healthy controls vs. burn patient group, **#** = significant difference between non-septic and septic burn patients. */# $p<0.05$, **/## $p<0.01$ and ***/### $p<0.001$.